LA-8715-PR

Progress Report

Space Nuclear Safety and Fuels Program

October 1980

LOS ALAMOS SCIENTIFIC LABORATORY
Post Office Box 1663 Los Alamos. New Mexico 87545

The four most recent reports in this series, unclassified, are LA-8573-PR, LA-8582-PR, LA-8713-PR, and LA-8714-PR.

This report was not edited by the Technical Information staff.

This work was supported by the US Department of Energy, Division of Space and Terrestrial Systems.

UNITED STATES
DEPARTMENT OF ENERGY
CONTRACT W-7405-ENG. 36

LA-8715-PR
Progress Report

UC-23
Issued: January 1981

Space Nuclear Safety and Fuels Program

October 1980

Compiled by

W. J. Maraman

ABSTRACT

This formal monthly report covers the studies related to the use of $^{238}PuO_2$ in radioisotopic power systems carried out for the Space and Terrestrial Systems Division of the U. S. Department of Energy by the Los Alamos National Laboratory.

Most of the studies discussed here are of a continuing nature. Results and conclusions described may change as the work continues. Published reference to the results cited in this report should not be made without the explicit permission of the person in charge of the work.

SPACE NUCLEAR SAFETY AND FUELS PROGRAM

OCTOBER 1980

Compiled by
W. J. Maraman

I. GENERAL-PURPOSE HEAT SOURCE (GPHS)

The remaining two tests in the Design Verification Test (DVT) series were completed this month, as were the metallographic examinations of the four iridium capsules used in the DVT series. The preliminary results of the four tests were reported at the International Solar-Polar Final Design Review held at the General Electric Corporation's Space Center, Valley Forge, Pennsylvania, October 28-30, 1980.

The DVT series was to have consisted of four tests, one sample impacted at 0^{o}, 27^{o}, 45^{o}, or 90^{o}. The test velocity was to be 58 mps, which is 110% of the expected sea-level terminal velocity of the ablated GPHS module. The impact temperature was to have been $820^{o}C$, the expected impact temperature. The first test (DVT-1), which was reported last month was performed at this temperature, but the remaining three tests were carried out at $850^{o}C$, by direction, because of the belief that the grain size data reported by us in the August Monthly Report would not apply to the current system.

Because of the failure in the 90^{o} test (DVT-2, IRG-88) that was reported last month, the fourth test, DVT-4, was performed as a repeat of DVT-2 (90^{o}) instead of at the originally intended 45^{o}.

A. Capsule Assembly IRG-89

This capsule assembly was impacted at 58 mps, $850^{o}C$, and 0^{o} (end-on) as part of the special half-module sample shown in Fig. 1. The aeroshell was machined slightly over half size, with a relief volume on one side of the graphite impact shell (GIS) location to simulate the internal crushup volume present in the GPHS module. The wall thicknesses were reduced 1.27 mm to simulate ablation losses. The insulation and impact-shell assemblies were normal, except for the following fueled clad, which was UO_2 in Pt-30 Rh.

The recovered test sample is shown in Fig. 2. The impacted end of the aeroshell was separated by the impact and the CBCF insulating disk was completely crushed. The impact assembly is shown in Fig. 3. It remained intact after the impact, but the impact end was delaminated and belled.

The recovered capsule, shown in Fig. 4, was deformed in the manner characteristic of the 0^{o} orientation in the current design of the GPHS module. No failures were visible.

B. Capsule Assembly IRG-90

This fueled clad was impacted at 58 mps and $850^{o}C$ in the 90^{o} orientation as part of sample DVT-4, which was a complete GPHS module. The aeroshell wall thicknesses were reduced 1.27 mm to simulate ablation and three of the fueled clads were simulated with UO_2 in Pt-30 Rh.

The pieces recovered from the impact catch tube are shown in Fig. 5 without the fueled clad, which was removed to the glove box. Both the aeroshell and the leading impact shell split longitudinally during the impact. Their respective end caps were also removed by that event.

The recovered fueled clad, IRG-90, is shown in Fig. 6. The general character of the deformation is quite similar to that of IRG-88, which was also impacted at 90° (September Monthly Report), but the deformations of the present capsule are less. All test conditions and sample components in the two 90° tests, DVT-2 and DVT-4, were as identical as possible. The results differed in the gross strains of the fueled clads and in the degree of graphite fragmentation. Qualitatively, the graphite in DVT-4 was the more damaged, which supports the idea that the deformation of the fueled clad is controlled by the balance of the impact resistances of the fuel and the crushing graphite.

C. Secondary Examinations of the DVT Fueled Clads

After recovery, the capsules from DVT-1, DVT-3, and DVT-4 (IRG-87, -89, and -90) were opened so that the fuel could be recovered for particle-size analyses. The fuel from IRG-88 (DVT-2) was not removed in the same manner, because of the failure of the clad. The split capsules with the fuel inside are shown in Fig. 7. The major fuel shear planes that controlled the local deformation offset in IRG-87 are readily apparent in Fig. 7a. Similar shear planes are visible in IRG-89 (Fig. 7b), but the full support provided by the aeroshell and impact shell in the end-on orientation prevented the differential movement necessary to cause the capsule offset. The fuel fragmentation in IRG-90, shown in Fig. 7c, was greater than that observed in either of the other orientations.

Full diametral-longitudinal sections of each of the fueled clads were cut, polished, and examined. These are shown in the photomacrographs of Fig. 8. The sections shown were not taken through the regions of maximum local strain, but were taken to illustrate the deformation in a plane of symmetry intersecting the impact target.

1. IRG-87. Figure 9 shows an etched cross section through the region of greatest offset, which demonstrates that, given the proper stress state, iridium can be quite ductile even at 820°C. The deformed grains are still visible, because the impact temperature was well below the recrystallization temperature. Figure 10 is an etched cross section from the trailing half of IRG-87, showing that even in a region of very low plastic strain of DOP-26 iridium is brittle if the stress state is tensile.

The grain size typical of IRG-87 is exemplified by the photomicrographs of Fig. 11, which shows a grain size of ~15 grains/thickness. The closure weld, shown in Fig. 12, was sound and had the proper microstructure and penetration.

2. IRG-88. The section through the major longitudinal crack is shown in Fig. 13 at low magnification and in Fig. 14, etched, at higher magnification. There is little or no evidence of plastic deformation in the iridium wall, except were a fuel fragment was pressed into the capsule, as seen in the right side of Fig. 14. This indicates that the present design of the GPHS module, with CBCF insulation, does not provide the needed support to the capsule during a 90° impact. Continued use of this design will require a significant temperature increase, if failures are to be eliminated.

In many areas, where the gross deformations were small, surface cracks like those shown in Fig. 10 were found in IRG-88. In addition, the internal

integranular crack, shown in Fig. 15 was found in IRG-88. Its orientation and location suggest that it was present in the capsule wall before the impact.

The microstructure of the closure weld is shown in Fig. 16. The weld was sound and of good quality before the impact, as demonstrated by the structure revealed in Fig. 16a. Figure 16b shows the weld in its failure region. The apparent large grains on the right of the photomicrograph result from incomplete etching of the general orientation and are not as large as they appear. The general grain size was again ~15 grains/thickness, which is normal for this heat treatment series, but, as Fig. 7 shows, the grain size is not uniform through the wall.

3. IRG-89. Although the local strains in the belled region of this capsule were relatively large (Fig. 4), the capsule did not fail. The reason for this is shown in Fig. 18, which is a section through this deformed region. The wall thickness in the bulged region is unthinned, perhaps even thickened, indicating that the net effective stress was compressive. No external surface cracks were observed in IRG-89, but the vent cover weld had failed, Fig. 19. This failure is of little consequence, but it illustrates the extreme sensitivity of coarse-grained iridium. The photomicrograph also illustrates the adjacency of the vent-cover and decontamination-cover welds. A design improvement would result if the latter were increased in diameter.

The closure weld in IRG-89 was of good quality and the general grain size was ~16 grains/thickness, a bit smaller than in IRG-87 or IRG-88.

4. IRG-90. Even though capsule IRG-90 sustained only modest strains during the impact and did not fail and release fuel, it contained several cracks on the impact face in the same general region as the longitudinal failures in IRG-88, which was also impacted in the 90° orientation. The worst of the cracks in IRG-90 is shown in Fig. 20. The crack had the usual integranular character and penetrated 90% of the wall thickness. Other, shallower, cracks were present on the impact face, too. The presence of these cracks in a sample with so little overall strain reinforces the argument that the CBCF design does not provide enough support to prevent failures. If the fuel or the impact shell and aeroshell had been less resistant, the iridium in IRG-90 would have failed.

The general grain size of IRG-90 was ~15 grains/thickness, but one region in the vented cup was significantly finer, ~20 grains/thickness. The closure weld structure was very good.

D. DVT Summary

The strains observed in the leading iridium capsules used in the DVT impact series are compared to those seen in three other comparable module impacts in Table I (local strains) and Fig. 21 (gross strains). It is unfortunate that there is no 90° test at the higher temperature to complete the comparison.

It does seem clear from the results of IRG-88 and IRG-90 that the CBCF-insulated design is vulnerable to impact failures in orientations close to 90° at the lower impact temperatures currently predicted. If it is not possible to raise the impact temperature significantly, it will be necessary to postulate in the safety analysis that some proportion of the impacting modules will fail and release fuel.

II. SYSTEMS SUPPORT

A. Stirling Isotope Power System

The accumulated exposure time for the 800°C test assembly was 24,958 h on November 1, 1980.

A gas-tap of the helium atmosphere of the test assembly was taken on October 8. Mass-spectrometric analysis indicated the presence of 40 ppm argon as the only detectable impurity. The detection limit for other permanent gases is about 50 ppm.

B. Iridium Impurity Effects

As a part of the continuing effort to assess the effect of phosphorous impurities on the grain growth of DOP-26 iridium, three samples of DOP-26 iridium have been annealed at 1330°C in a graphite container with P_2O_5 for 500, 2000, and 3000 h, respectively. The grain sizes, together with the available Auger electron spectroscopy (AES) analysis results, are summarized in Table II. The available AES analysis results, are summarized in Table II.

The grain size of the specimen treated for 500 h fits the data previously obtained for phosphorous-doped material. However, the grain sizes of the 2000 h and 3000 h specimens are smaller than predicted for phosphorous-doped material, but larger than indicated by Oak Ridge National Laboratory (ORNL) studies on DOP-26 iridium.

The specimens used in this experiment were taken from scraps obtained from sheet supplied by ORNL, from which tensile specimens used in the PuO_2 compatibility series had been fabricated. Some of the tensile specimens had much smaller than expected grain sizes following the compatibility exposure. It thus appears that the 2000 and 3000 h phosphorous-doped specimens were identical to the tensile specimens, which yielded the smaller-than-expected grain size. The results suggest that this material was not typical, and perhaps may have been an entirely different alloy. The two metallographic samples of the phosphorous-doped material along with an additional untreated sample have been sent to ORNL for SSMS analysis to determine if the thorium content is indeed representative of DOP-26 iridium. No results have been obtained from ORNL.

The exposure of an unfueled DOP-26 iridium post-impact containment shell (PICS) contained in a multi-hundred watt (MHW) impact shell at 1330°C has been terminated after 4000 h . The grain size of the hemispheres, as determined by a grain intercept technique, was 14.1 and 14.8 grains/thickness. These results are consistent with expected grain growth based on ORNL studies for DOP-26 iridium and do not indicate any enhanced grain growth of the iridium PICS as a result of exposure in contact with a MHW impact shell.

III. LIGHT-WEIGHT RADIOISOTOPE HEATER UNIT (LWRHU)

A. Design

Mound Facility (MF) drawings for the insulator components and graphite parts assembly were reviewed, checked against the Los Alamos National Laboratory test component drawings, and approved for production. D. Galvin, MF, and R. Tate, Los Alamos, agreed that the best way to solve problems that might arise from lack of concentricity in the pyrolytic graphite tubes was to specify that all finished tubes must have complete stand-off rings with a minimum height of 0.025 mm and that the end caps must be preassembled with the

tube nest prior to acceptance. Selective assembly was deemed more practical than stringent concentricity specifications on the vendor's product.

An Engineering Change Request to establish a lower particle size limit and a higher, but more realistic, impurity level in the platinum frit powder, was reviewed and approved.

Four Materials Review Board actions were reviewed and approved. These included the following:

1. Seven clad bodies with slightly out-of-tolerance dimensions in noncritical areas were recommended for acceptance.
2. Three closure caps with slightly out of tolerance dimensions of the slots were recommended for acceptance.
3. Rewelding of the vent end caps in nine subassemblies was recommended for acceptance.
4. An aeroshell body with an internal stand off slightly off the specified diameter was recommended for acceptance.

B. Reentry

The residual helium in the fuel from LWRHU capsule RHU027 after it was exposed to a reentry ramp was 0.64 cc/g, equal to 1.3 cc in the 2.1 g pellet. Between the reentry exposure and the analysis, 0.15 cc was generated, so 1.15 cc remained in the pellet after the reentry. This means that ~86% of the original content of 8.46 cc was released during the reentry. Our calculated value was 95%.

IV. TECHNOLOGY

Compression tests of $^{239}PuO_2$ samples containing 1.3 mol% Y_2O_3, La_2O_3, or Nb_2O_5 were carried out at 1150°C. No significant ductility increases were observed for any of the samples, although the Nb_2O_5 specimen showed the highest value of the three. Results of all tests performed to date are shown in Table III. For comparison, $^{239}PuO_{1.90}$ produced by graphite die reduction during hot pressing had a yield stress of 140 MPa with 14% strain, while $^{239}PuO_{2.00}$ stoichiometric material showed a yield stress of 210 MPa with 4% strain, these data are also for 1150°C.

Metallographic examinations of untested companion pellets revealed the presence of numerous small cracks. These appear to have been caused by excess pressure during the cold pressing step in fabrication. Four additional pellets containing 1.3 mol% Nb_2O_5 were made using 13.8 MPa for cold pressing.

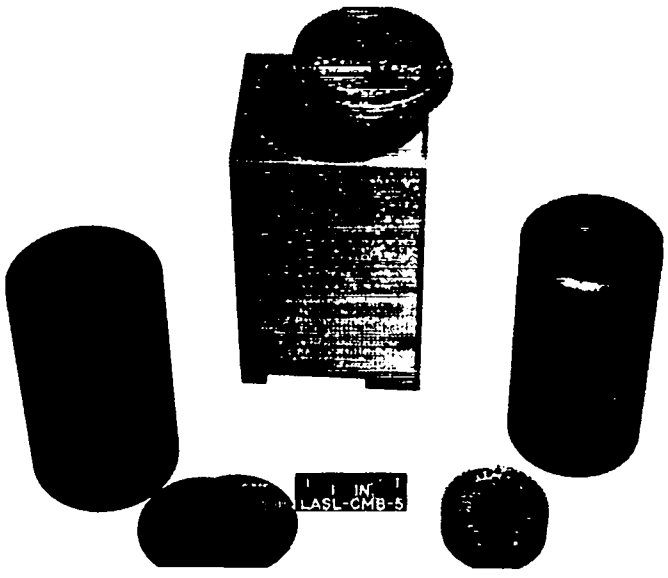

Fig. 1.

The 0° impact of IRG-89 (DVT-3) was accomplished by a special half-module.

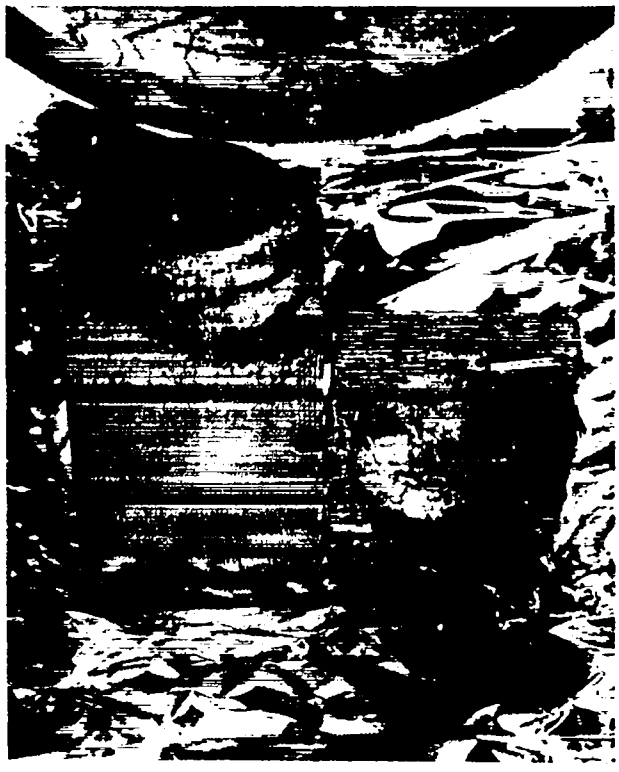

Fig. 2.

Test assembly DVT-3 (IRG-89) after impact. The fueled clad remained contained.

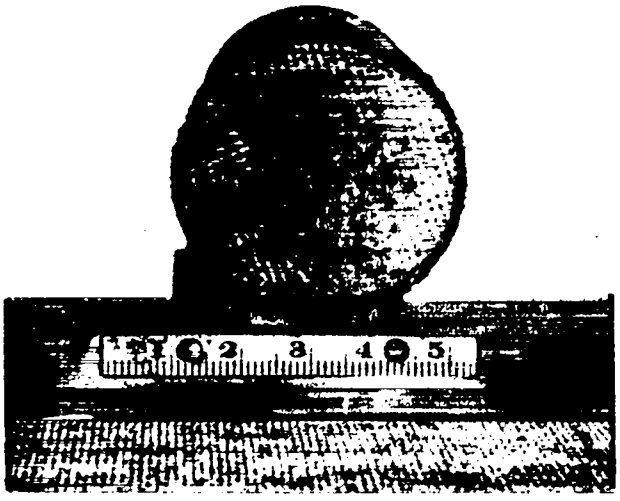

(a)

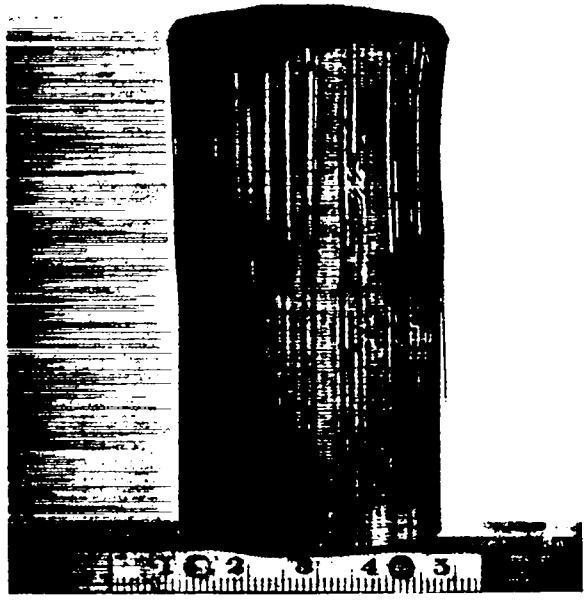

(b)

Fig. 3.

The impact assembly from test DVT-2 (IRG-89) was intact when recovered. a) The CBCF end-disk was completely crushed and pushed into the holes in the end of the impact shell. b) The impact shell's body was cracked and belled by the impact.

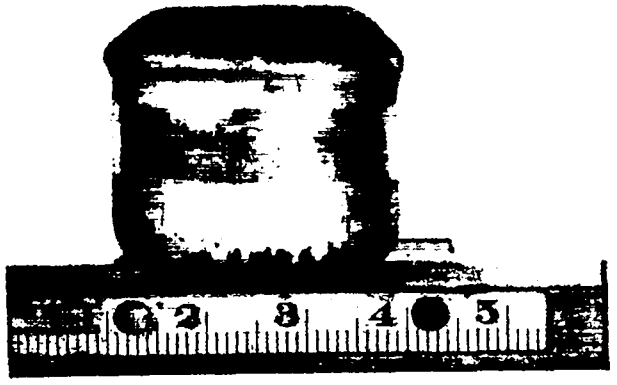

Fig. 4.
The fueled clad from DVT-3 (IRG-89) was deformed by the impact, but did not fail.

Fig. 5.
The graphite components of sample DVT-4 (IRG-90) were damaged significantly by the impact. The fueled clad, which had been removed before this photograph was made, was deformed, but had not released any fuel.

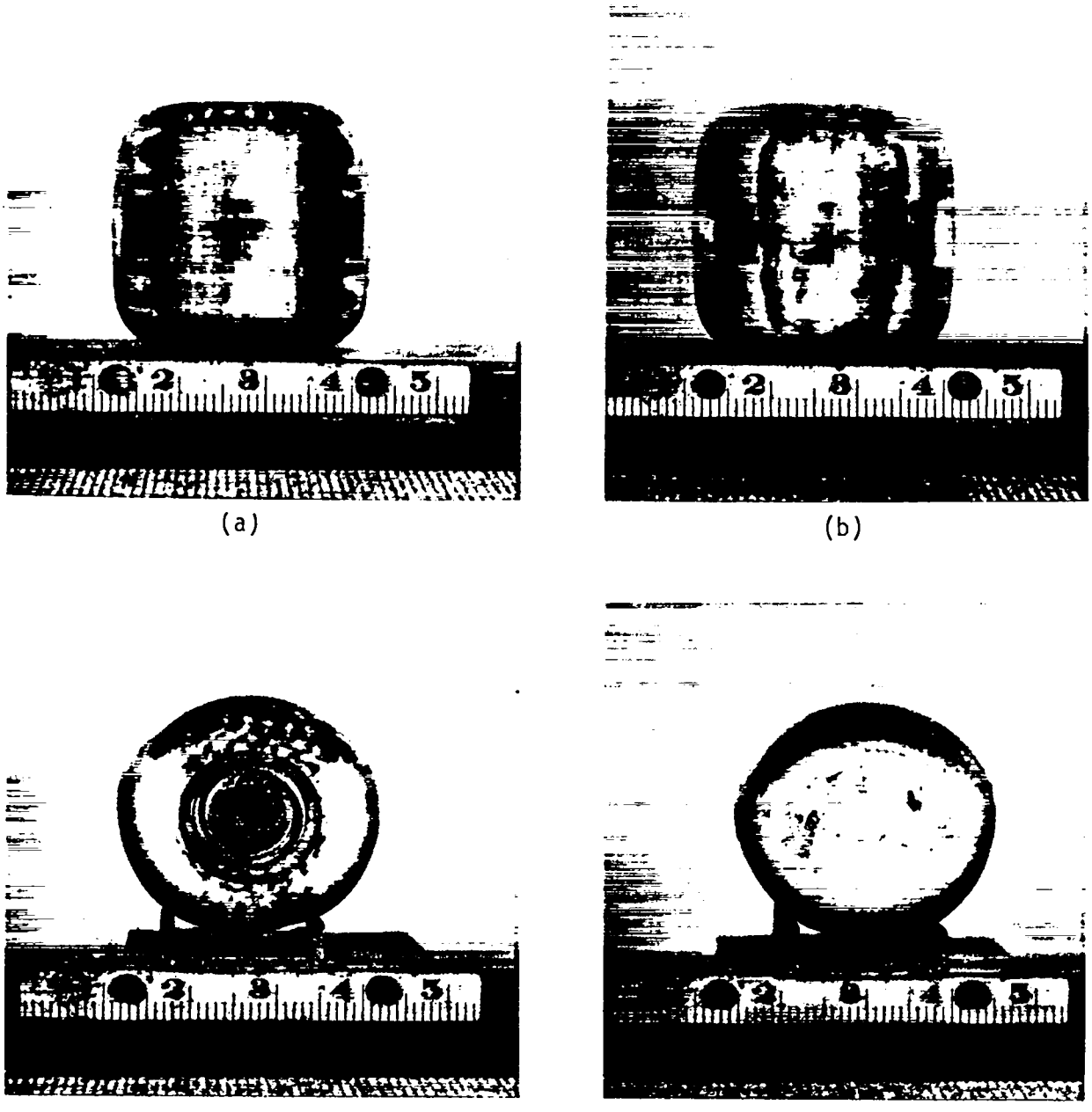

Fig. 6.
The fueled clad from DVT-4 (IRG-90) was not deformed severely by its impact. a) Impact face; b) trailing side; c) vent end; and d) plain end.

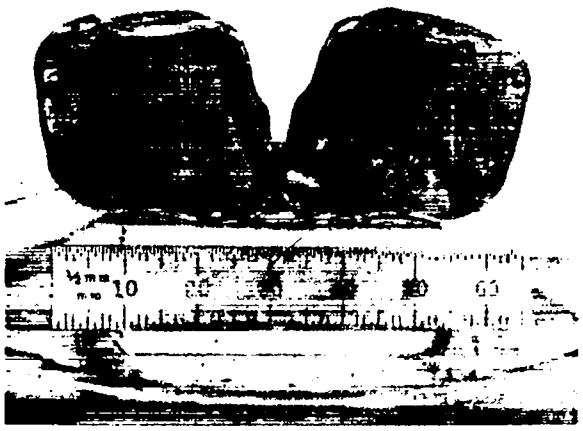

(b)

(c)

Fig. 7.
After the iridium capsules were cut open, the degree of fuel fracture was evident. a) IRG-87; b) IRG-89, and c) IRG-90.

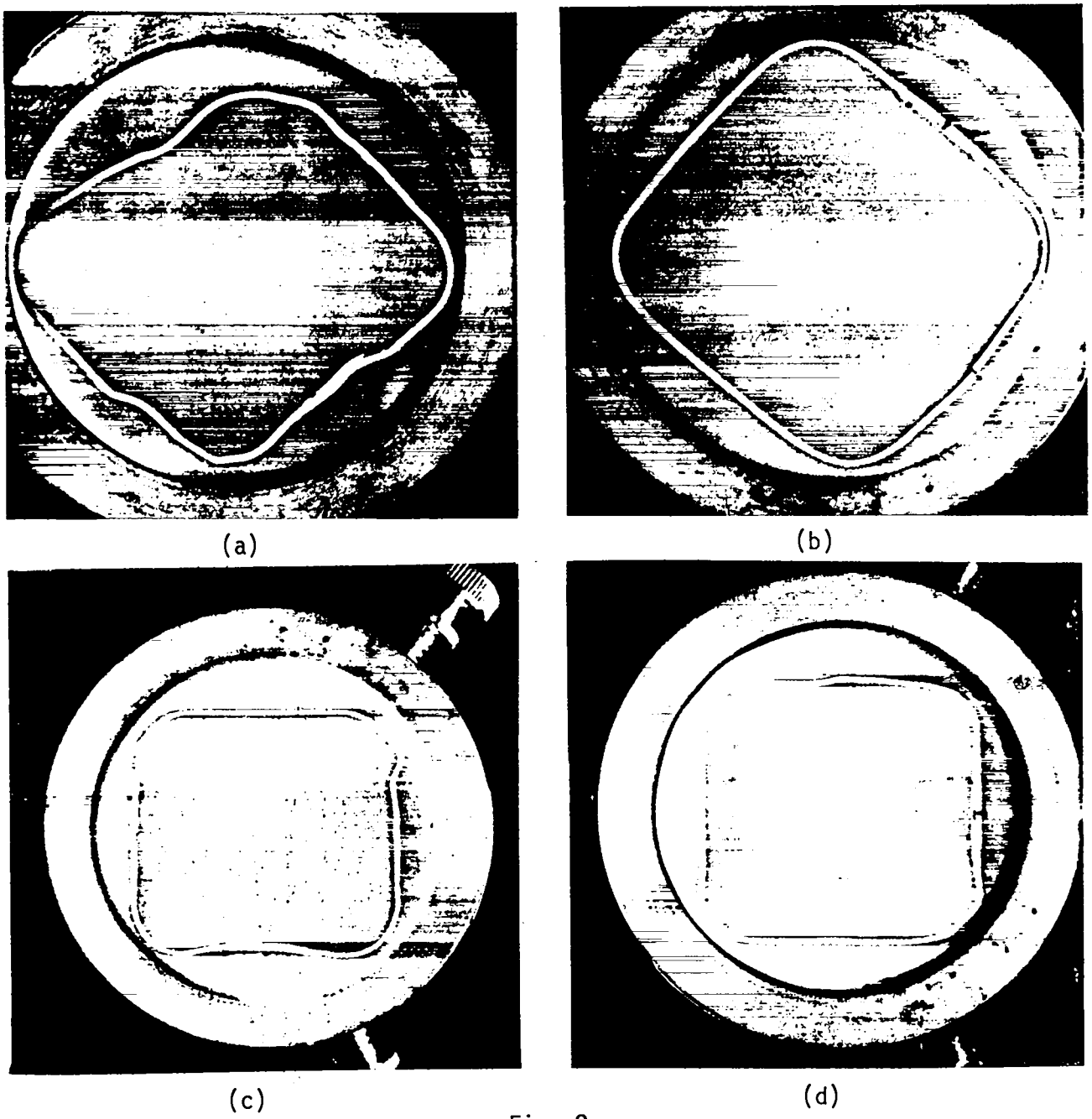

Fig. 8.
Cross sections of the iridium capsules used in the DVT impacts. a) IRG-87, 27°; b) IRG-88, 90°; c) IRG-89, 0°; and d) IRG-90, 90°.

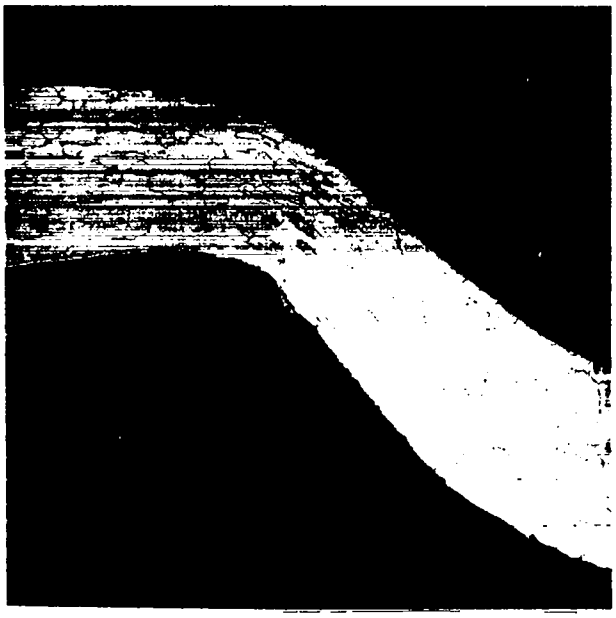

Fig. 9.
The impact face of IRG-87 sustained large plastic strains without failing. 50X.

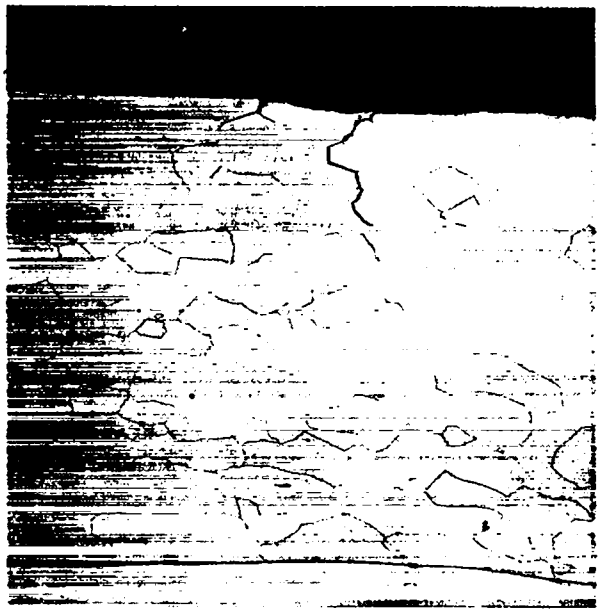

Fig. 10.
The trailing end of IRG-87 cracked at very low strains. 100X.

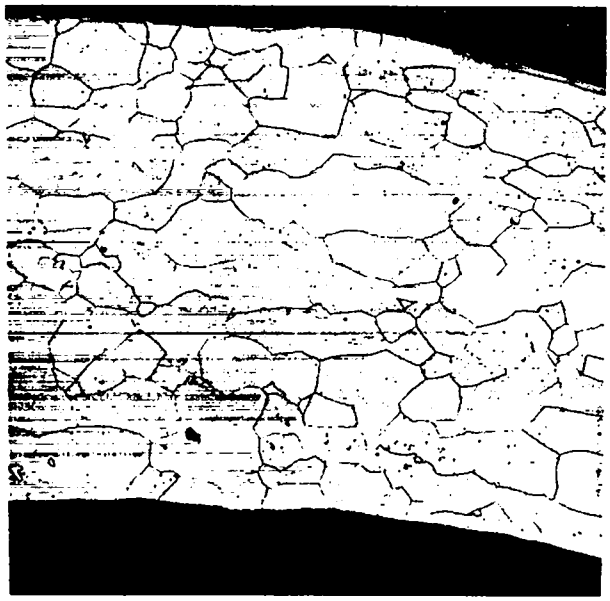

Fig. 11.
The etched section of IRG-87 revealed a grain size of ~15 grains/thickness. 100X.

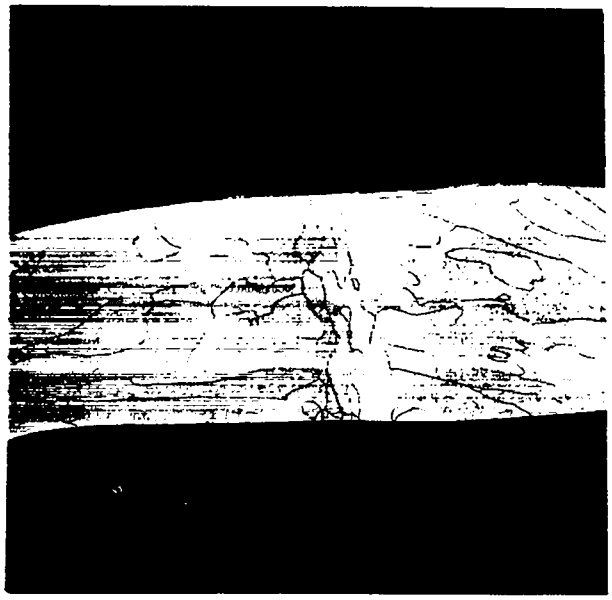

Fig. 12.
The closure weld of IRG-87 was completely satisfactory. 50X.

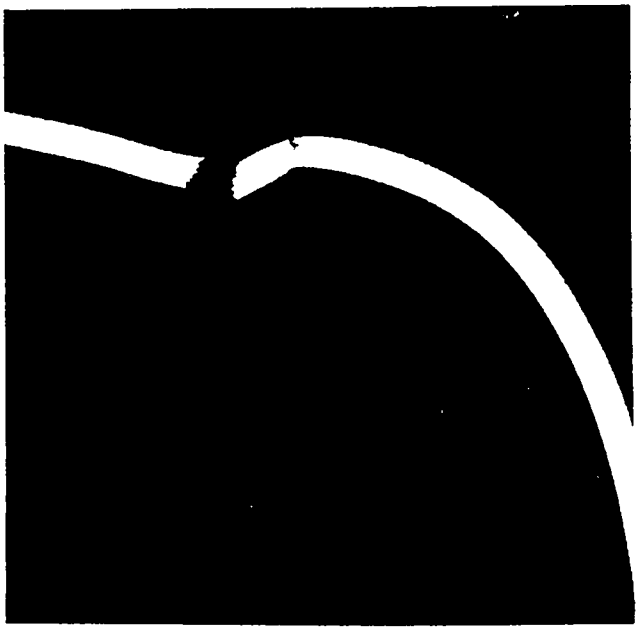

Fig. 13.
The major longitudinal fracture on the impact face of IRG-88. 7X.

Fig. 14.
The failures in IRG-88 were all in the form of grain boundary cracks. 40X.

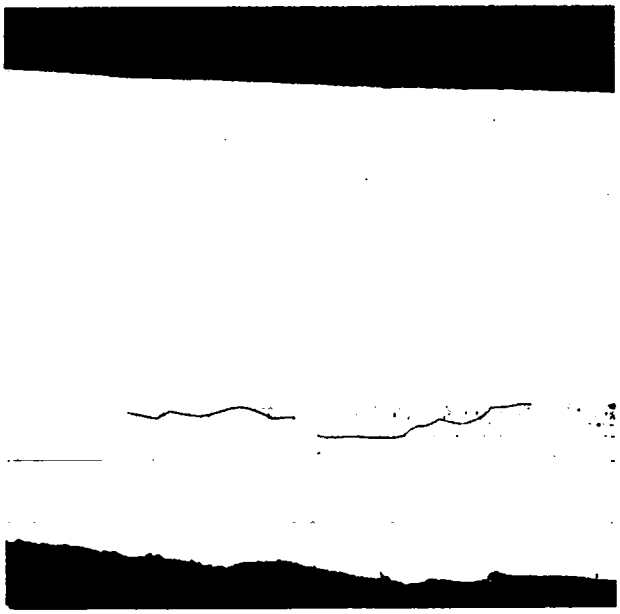

Fig. 15.
An internal intergranular crack was observed in IRG-88. 100X.

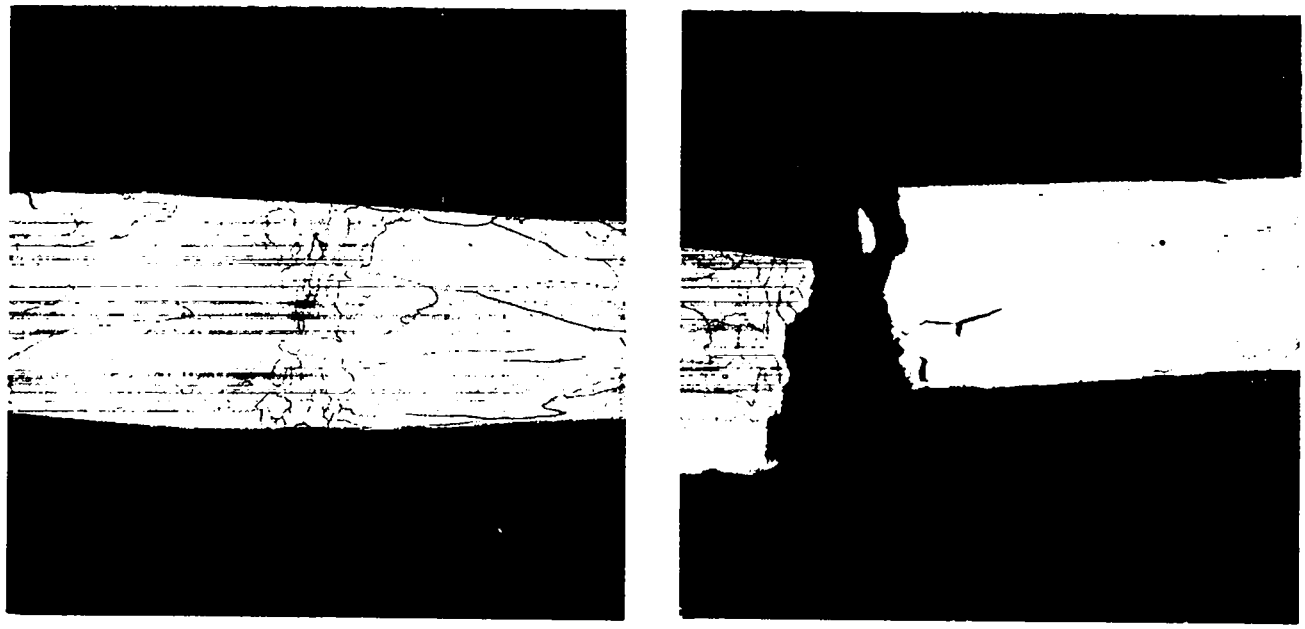

(a) (b)

Fig. 16.
The weld microstructure of IRG-88 was normal. The failure shown in (b) is thought to be a secondary crack propagated after the longitudinal primary crack was formed. 40X.

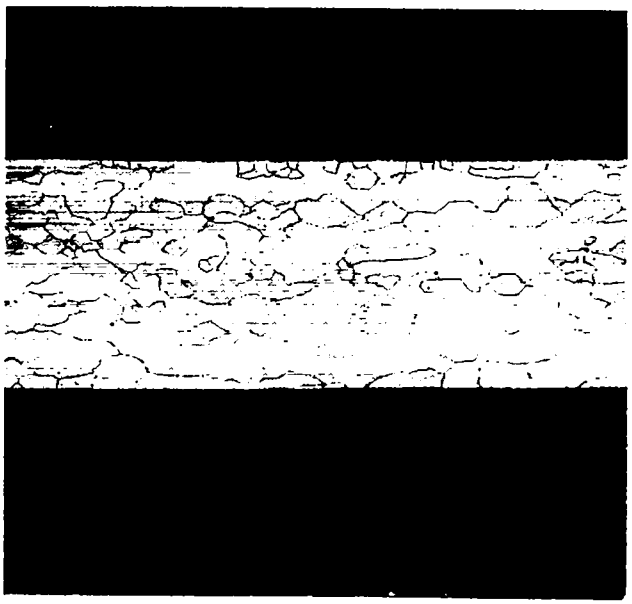

Fig. 17.
The grain size of IRG-88 was ∿15 grains/ thickness, but there is some evidence of a size gradient in the capsule wall. 50X.

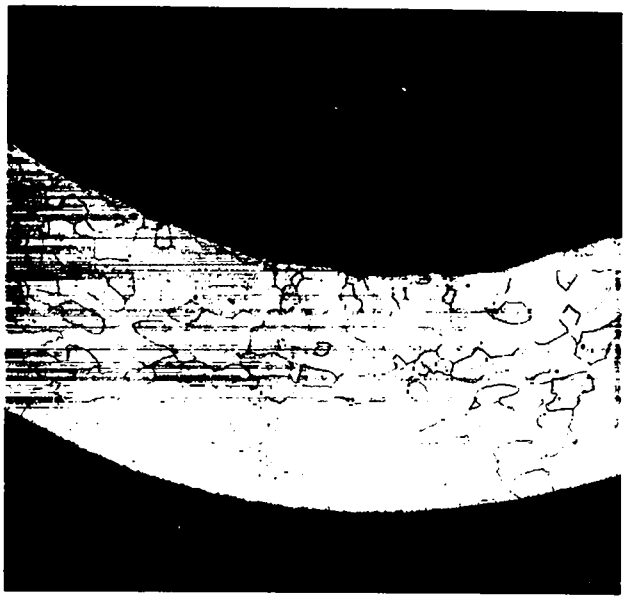

Fig. 18.
The belled region in IRG-89 was not thinned during its deformation and did not fail. 50X.

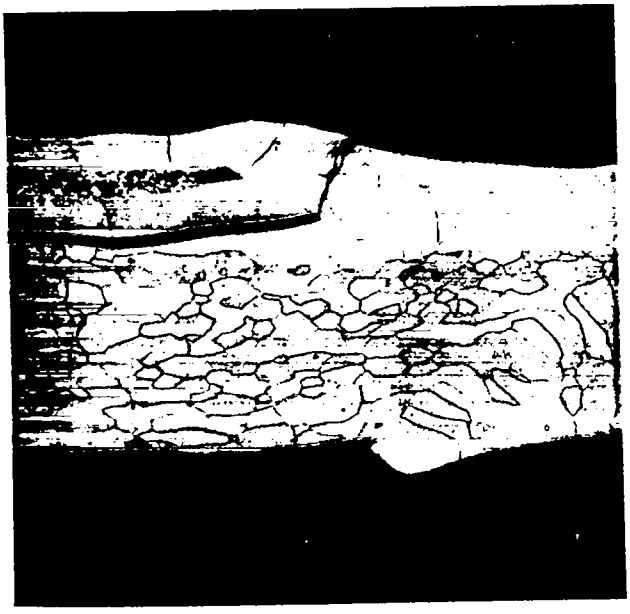

Fig. 19.
The vent assembly weld of IRG-89 was cracked after the impact. 50X.

Fig. 20.
The wall of IRG-90 was nearly penetrated by a longitudinal crack on the impact face. 100X.

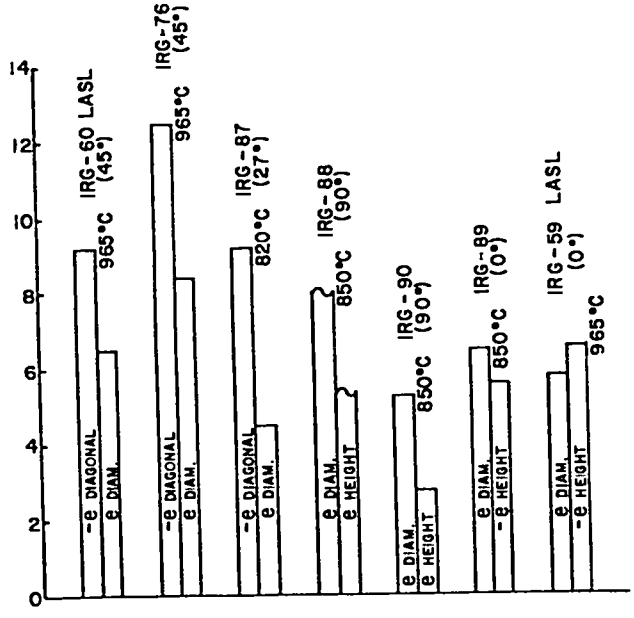

Fig. 21.
Major clad strains observed after module impact tests.

TABLE I

MODULE IMPACTS
LOCAL BENDING STRAIN %

CAPSULE #	FUEL	IMPACT TEMPERATURE °C	ORIENTATION °	LOCAL STRAIN MAX. % BEND
IRG-59	LASL	965°	0°	10.1
IRG-60	LASL	965°	45°	12.9
IRG-76	SRL	965°	45°	16.1
IRG-87	SRL	820°	27°	17.6*
IRG-88	SRL	850°	90°	FAILED
IRG-89	SRL	850°	0°	14.1
IRG-90	SRL	850°	90°	2.5

NOTES: ALL MODULES IMPACTED AT 58 m/s

*SECTIONED VALUE. PRIOR ESTIMATE 16.1 % FROM EXTERNAL BEND.

TABLE II

GRAIN SIZE AND AES RESULTS OF PHOSPHOROUS-DOPED DOP-26 IRIDIUM

Exposure	Grain Size	Location	Th_{65}/Ir_{229}	P_{120}/Ir_{229}
500 hours @ 1330°C w/P_2O_5	14.9 gr/thk.	Edge	0.94	0.63
		Center	0.91	0.56
		Edge	1.18	0.81
2000 hours @ 1330°C w/P_2O_5	10.6 gr/thk.	Edge	1.21	0.50
		Center	1.13	0.56
		Edge	0.14	0.20
3000 hours @ 1330°C w/P_2O_5	10.1 gr/thk.	Not available		

TABLE III

COMPRESSION TESTS AT 1500°C

Test #	Specimen #	Alloying Addition (mole %)	L/O Ratio	Yield Stress (MPa)	Ultimate Stress (MPa)	Strain at Ultimate Stress	Strain on Sample * After Test	Strain Rate (s^{-1})
PuO_2-1	17108-21C	10% Y_2O_3	0.93	447	447	0.21%	Specimen Shattered	1.2×10^{-4}
PuO_2-2	17108-21B	10% Y_2O_3	0.98	356	356	0.20%	Specimen Shattered	8.7×10^{-5}
PuO_2-3	17108-19	5% Y_2O_3	1.26	65.7	65.7	0.30%	Specimen Shattered	6.5×10^{-5}
PuO_2-4	17108-26A	1.3% Y_2O_3	1.04	227	227	0.25%	2.3%	1.0×10^{-4}
PuO_2-5	17108-27A	1.3% La_2O_3	1.47	66.6	66.6	0.46%	1.2%	7.6×10^{-5}
PuO_2-6	17108-29A	1.3% Nb_2O_5	1.57	79.5	81.7	0.83%	3.3%	6.9×10^{-5}

* Specimens showed surface cracking and spalling, but enough of the pellet was still intact to allow for a length measurement. These specimens were unloaded after the maximum load was attained but, before reaching zero load.

ADDITIONAL DISTRIBUTION

B. J. Rock, Dept. of Energy/ANSP, Washington, DC
G. L. Bennett, Dept. of Energy/ANSP, Washington, DC
T. J. Dobry, Dept. of Energy/ANSP, Washington, DC
J. J. Lombardo, Dept. of Energy/ANSP, Washington, DC
R. B. Morrow, Dept. of Energy/ANSP, Washington, DC
C. O. Tarr, Dept. of Energy/ANSP, Washington, DC
R. Brouns, Dept. of Energy/ANSP, Washington, DC
J. Griffo, Dept. of Energy/ANSP, Washington, DC
J. L. Liverman, Dept. of Energy/ANSP, Washington, DC
R. Ferguson, Dept. of Energy/ET, Washington, DC
D. K. Stevens, Dept. of Energy/BES, Washington, DC
H. E. Roser, Dept. of Energy/ALO, Albuquerque, NM
J. A. Morley, Dept. of Energy/ALO, Albuquerque, NM
D. L. Plymale, Dept. of Energy/ALO, Albuquerque, NM
H. N Hill, Dept. of Energy/DOA, Miamisburg, OH
M. J. Sires, Dept. of Energy/SRO, Aiken, SC
R. J. Hart, Dept. of Energy/ORO, Oak Ridge, TN
W. L. Von Flue, Dept. of Energy, SFOO, Oakland, CA
T. B. Kerr, NASA, Washington, DC
R. A. Ivanoff, NASA/JPL, Pasadena, CA
G. Stapfer, NASA/JPL, Pasadena, CA
R. Campbell, NASA/JPL, Pasadena, CA
AFISC/SNS, Attn: Col. J. A. Richardson, KAFB, Albuquerque, NM
AFWL/NTYVS, Attn: Capt. J. D. Martens, KAFB, Albuquerque, NM
HQ Space Div./YLVS: Attn: Lt. Col. Needham, Los Angeles, CA
R. L. Folger, SRL, Aiken, SC
R. H. Tait, SRL, Aiken, SC
J. B. Mellen, SRP, Aiken, SC
G. W. Wilds, SRP, Aiken, SC
R. A. Brownback, SRP, Aiken, SC
J. R. McClain, MRC, Miamisburg, OH
W. T. Cave, MRC, Miamisburg, OH
B. T. Kokenge, MRC, Miamisburg, OH
E. W. Johnson, MRC, Miamisburg, OH
H. Postma, ORNL, Oak Ridge, TN
A. C. Schaffhauser, ORNL, Oak Ridge, TN
H. Inouye, ORNL, Oak Ridge, TN
E. Foster, BCL, Columbus, OH
I. Grinberg, BCL, Columbus, OH
C. Alexander, BCL, Columbus, OH
E. E. Rice, BCL, Columbus, OH
J. Hagan, APL, Baltimore, MD
R. W. Englehart, NUS Corp., Rockville, MD
H. H. Van Tuyl, PNL, Richland, WA
A. Schock, Fairchild-Hiller Ind., Germantown, MD
C. W. Whitmore, GE, Philadelphia, PA
R. Hemler, GE, Philadelphia, PA
V. Haley, GE, Philadelphia, PA
E. C. Krueger, Sundstrand, Rockford, IL
F. Schumann, TES, Timonium, MD
J. Boretz, TRW, Redondo Beach, CA
R. Hartman, GE, Philadelphia, PA

W. Mecham, ANL, Argonne, IL
G. A. Cowan, Los Alamos, NM
R. D. Baker, Los Alamos, NM
R. N. R. Mulford, Los Alamos, NM
W. F. Miller, Los Alamos, NM
R. J. Pryor, Los Alamos, NM
G. R. Waterbury, Los Alamos, NM
R. Behrens, Los Alamos, NM
S. E. Bronisz, Los Alamos, NM
R. V. Browning, Los Alamos, NM
R. A. Kent, Los Alamos, NM
W. Stark, Los Alamos, NM
R. W. Zocher, Los Alamos, NM

Printed in the United States of America
Available from
National Technical Information Service
US Department of Commerce
5285 Port Royal Road
Springfield, VA 22161

Microfiche $3.50 (A01)

Page Range	Domestic Price	NTIS Price Code	Page Range	Domestic Price	NTIS Price Code	Page Range	Domestic Price	NTIS Price Code	Page Range	Domestic Price	NTIS Price Code
001-025	$ 5.00	A02	151-175	$11.00	A08	301-325	$17.00	A14	451-475	$23.00	A20
026-050	6.00	A03	176-200	12.00	A09	326-350	18.00	A15	476-500	24.00	A21
051-075	7.00	A04	201-225	13.00	A10	351-375	19.00	A16	501-525	25.00	A22
076-100	8.00	A05	226-250	14.00	A11	376-400	20.00	A17	526-550	26.00	A23
101-125	9.00	A06	251-275	15.00	A12	401-425	21.00	A18	551-575	27.00	A24
126-150	10.00	A07	276-300	16.00	A13	426-450	22.00	A19	576-600	28.00	A25
									601-up	†	A99

†Add $1.00 for each additional 25-page increment or portion thereof from 601 pages up.